JOURNAL OF AIRCRAFT
Vol. 42, No. 6, November–December 2005

In-Flight Thrust Measurements of Propeller-Driven Airplanes

Mehdi Sabzehparvar*
Amirkabir University of Technology, 15875-4413 Tehran, Iran

The development of a propeller model that will accurately predict airplane engine static and dynamic thrust and torque in a full range of advance ratio has provided a powerful and reliable source for propeller-driven airplane engine simulation that serves as a valuable tool for flight test analysis. A single-element propeller model that reduces the propeller characteristics to a lift and drag coefficient vs angle-of-attack formulation was found to describe accurately the propeller characteristics over a wide operating range. Measurements of airplane indicated airspeed, flight altitude, torque, propeller speed, and throttle setting are the only required parameters for in-flight thrust estimation. A check of the model showed that the predicted and measured values of static thrust, torque, and dynamic thrust were within less than 2% over a wide range of advance ratios. With an accurate model of in-flight thrust measurement, one could add a new gage on propeller-driven airplane to display the amount of available thrust for the pilot or autopilot system, which would have a great impact on both the capability of verifying airplane's maneuvers and flight safety during recovery procedures.

Nomenclature

A_I	=	propeller model parameter set
C	=	propeller blade chord
C_{Db}	=	propeller blade drag coefficient
C_{Lb}	=	propeller blade lift coefficient
C_P	=	power coefficient
C_Q	=	torque coefficient
C_T	=	thrust coefficient
J	=	advance ratio, 101.34 (V/nD)
N_B	=	number of propeller blades
n	=	speed, rpm
P_s	=	shaft power
Q	=	shaft torque
R	=	propeller radius
r	=	propeller blade element radius
s	=	solidity ratio
T	=	engine thrust
x	=	r/R
α_b	=	blade angle of attack
θ	=	blade angle
ρ	=	air density
ω	=	propeller rotational speed, rpm

Introduction

THERE have always been difficulties in separating thrust and drag forces acting on a propeller-driven airplane. The usual flight-test method[1] used to determine airplane drag is to generate a power-required curve for the airplane. The engine shaft power is measured using calibration curves or a torque meter is installed and airspeed is varied incrementally over the performance envelope of the airplane. A propeller efficiency is assumed using the Hamilton standard method[2] or a propeller chart. Hewes rediscovered Lock's model for propeller thrust and shaft power (Hewes, D. E., and Bennett, A. G., private discussion on propeller modeling employing Lock's method, 1981). It was obvious that the propeller characteristics could be modeled as functions that would suitable for parameter identification methods.

Lock conducted extensive propeller research during the 1930s and 1940s. As part of his work, he developed a single-element model[3–6] for propeller thrust and shaft power that is based on the concept that equivalent propeller lift and drag polars are functions of the blade angle of attack at the 0.7 propeller radius that is applicable for any blade angle and advance ratio. The simplified model was found to be robust due to the inclusion of Goldstein terms to account for interference velocity due to multiple blades. The direct method computes the propeller thrust and shaft power assuming the propeller lift and drag polar are defined.

Of particular interest was the inverse method, which has been developed to compute the equivalent blade lift coefficient C_{Lb} and blade drag coefficient C_{Db} given measured propeller advance ratio, thrust, and shaft power. Haines[7] conducted an extensive study of the lift and drag polar of propellers using Lock's inverse method. It was found that the equivalent blade lift polar exhibited a linear range and a smooth transition into a stalled regime. Similarly the equivalent drag polar was found to be parabolic. It was shown that these polars were universal for a wide range of blade angles and advance ratios. The propeller blade polar was shown to depend on the tip Mach number when the tip Mach number was in excess of 0.8. It was obvious that the propeller blade polar exhibited characteristics similar to that of an airplane; thus, the polar could be fitted with low-order polynomials that would be suitable for completing the performance model for a propeller-driven airplane.

The discussion that follows adopts briefly the development of a propeller performance analysis method using Lock's propeller model. The fundamental approach is to optimize propeller blade angle of attack to minimize the differences between calculated and measured values of engine torque at each flight setting. Once the propeller blade angle-of-attack adjustment in the model has reached its optimized point, the calculated value of thrust could be adopted as in-flight thrust measurement value.

Theory

The discussion of the theoretical aspects of the method will consider some details of Lock's propeller model and the basis for the adoption of this method to predict propeller thrust and shaft power.

Lock's Propeller Model

The direct, single-element propeller model assumes that the blade lift and drag coefficients acting at $0.7R$ can be used to represent the entire propeller if the appropriate integrating factor is used. The definitions of the force directions and the velocity components are shown in Fig. 1. It is assumed that the aerodynamic forces are aligned with the local relative wind as is done in wing lifting line theory. The application of the Lock's simplified method of integration yields the

Received 14 August 2004; revision received 1 December 2004; accepted for publication 7 December 2004.

*Assistant Professor, P.O. Box 15875-4413, Aerospace Department, 424 Hafez Avenue; sabzeh@cic.aut.ac.air.

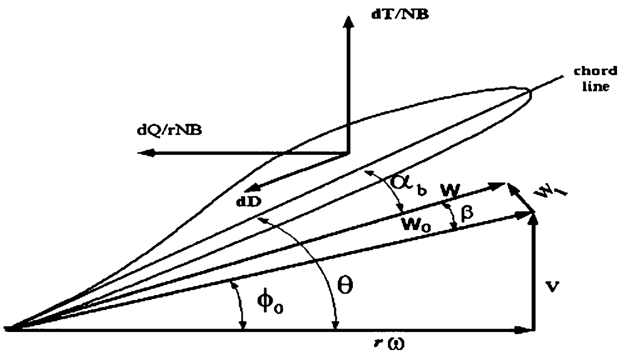

Fig. 1 Forces and velocity vectors for a propeller blade element.

following expression for propeller thrust with the variables evaluated at $0.7R$:

$$T = 0.5\rho N_B C W^2 R X [C_{\text{Lb}} \cos(\phi) - C_{\text{Db}} \sin(\phi)] \tag{1}$$

where

$$\phi = \theta - \alpha_b \tag{2}$$

The key to this method is the calculation of the induced velocity w_1 and the blade angle of attack α_b. The following are some relationships and definitions:

$$W^2 = W_0^2 - W_1^2 \tag{3}$$

$$W_0^2 = r^2\omega^2 + V^2 \tag{4}$$

Also,

$$W_1 = W_0 \sin(\beta) \tag{5}$$

where

$$\beta = \theta - \alpha_b - \phi_0 \tag{6}$$

Calculation of the blade angle of attack is described later. The angle ϕ_0 is defined using Fig. 1,

$$\phi_0 = A \tan(V/r\omega) = A \tan(J/\pi X) \tag{7}$$

When the definition of J is included and factoring, the section total and induced velocities can be written in terms of the forward speed and advance ratio as

$$W = V_c^{0.5} V \cos(\beta) \tag{8}$$

$$W_1 = V_c^{0.5} V \sin(\beta) \tag{9}$$

$$V_C = (1 + \pi^2 x^2 / J^2) \tag{10}$$

Substitution of the preceding relationships allow expression (1) to be written as

$$T = 0.5\rho N_B C V_c V^2 R X \cos^2(\beta)[\cos(\phi) C_{\text{Lb}} - \sin(\phi) C_{\text{Db}}] \tag{11}$$

The calculation of the blade angle of attack requires an iterative procedure to determine α_b that will satisfy the simultaneous equations

$$s C_{\text{Lb}} = 4\chi \sin(\phi)\tan(\beta) \tag{12}$$

$$s C_{\text{Lb}} = f(\alpha_b) \tag{13}$$

where Eq. (12) is the induced velocity equation and Eq. (13) is the blade lift polar defined using analysis or the inverse method discussed later. Equation (11) was evaluated using a table lookup routine for the tip loss factor χ, which is a function of advance ratio j and the parameter ϕ.

The shaft power equation is also developed by referring to Lock,[6] where

$$P_S = \omega Q = T V + P_1 + P_2 \tag{14}$$

where P_1 is the induced power loss and P_2 is the profile drag power loss. After some manipulation P_1 is defined as

$$P_1 = \frac{V_c T V \sin(\beta)}{\cos(\theta - \alpha_b)} \tag{15}$$

and P_2 can be written as

$$P_2 = 0.5\rho N_B C W^2 R X C_{\text{Db}} \tag{16}$$

The shaft power can be written in a form similar to the thrust equation (11) after some algebra as

$$P_S = 0.5\rho N_B C R X V^3 \cos^2 V_C \big\{[C_{\text{Lb}} \cos(\beta) - C_{\text{Db}} \sin(\phi)] \times [1 + V_C \sin(\beta)/\cos(\phi)] + V_C^{0.5} \cos(\beta) C_{\text{Db}}\big\} \tag{17}$$

Inverse Method and Propeller Blade Polar Models

The inverse method developed by Lock[6] to compute the equivalent blade lift and drag coefficients and angle of attack is briefly summarized and applied to measured propeller–nacelle data to verify the method. When it is assumed that propeller thrust, shaft power, and advance ratio have been measured, the direct method can be inverted to yield expressions for blade lift and drag coefficients C_{Lb} and C_{Db} defined to be

$$C_{\text{Lb}} = [E C_T \cos(\phi) + F C_Q \sin(\phi)]/s \tag{18}$$

$$C_{\text{Db}} = [F C_Q \cos(\phi) - E C_T \sin(\phi)]/s \tag{19}$$

where E and F are the average values of the integrating factor as given in Ref. 7 by

$$E = \frac{3.276}{4.336 + J^2}, \qquad F = \frac{2E}{X} \tag{20}$$

When this formula and the standard radius at the value of $x = 0.7$, which is related to the shape of thrust grading curve as described in Ref. 6, are used, blade element lift and drag coefficients are obtained by the analysis of actual measurements of thrust and torque.

Because the blade angle of attack can not be measured directly, two separate equations for the blade lift coefficient were used to solve for the angle α_b. Two equations given by Lock for the blade lift coefficient are

$$s C_{\text{Lb}} = 4\chi \sin(\phi)\tan(\beta) \tag{21}$$

$$s C_{\text{Lb}} = E C_T \cos(\phi) + F C_Q \sin(\phi) \tag{22}$$

which require an iterative solution for α_b. The table lookup procedure described for the direct method is used for the inverse method as well.

Data[8] from a propeller test, which was not included in the Haines[7] study was processed using the inverse method to develop blade lift and drag polar. The test used a full-scale propeller with a Royal Air Force-(RAF-) 6 section and was installed in a realistic nacelle. Thrust and shaft power measurements of a wide range of propeller blade angles and advance ratio were used to explore the capability of the method to reduce the data to lift and drag polar. The polars that are produced by Lock's method are shown in Figs. 2–4. It is clear from comparisons with curve fits that the data for a wide range of blade angles can be reduced to lift and drag polar with very little scatter. However, note that the tip Mach numbers for this propeller test were always below 0.7. Inspection of the lift polar showed a linear region and a smooth transition into a stall. A single function will not fit the curve well, and so a two-segment model for the lift polar was assumed.

A first-order function of

$$C_{\text{Lb}_1} = A_1 + A_2 \alpha_b, \qquad (\alpha < \alpha_{\text{bp}}) \tag{23}$$

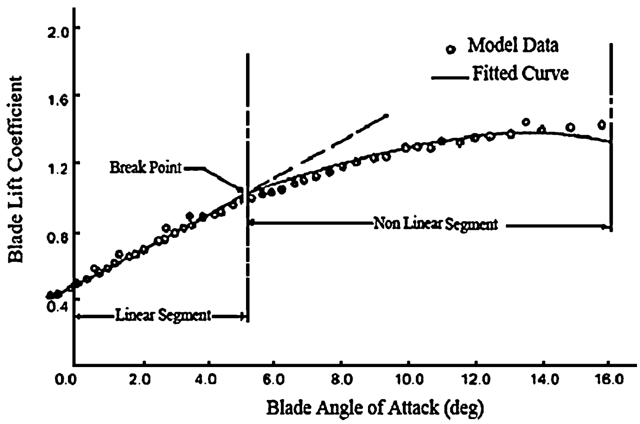

Fig. 2 Blade lift coefficient vs angle of attack.

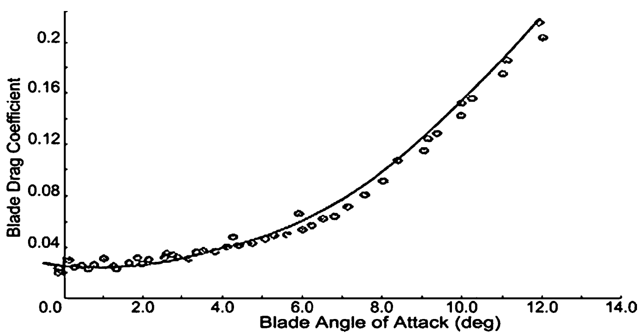

Fig. 3 Blade drag coefficients vs blade angle of attack.

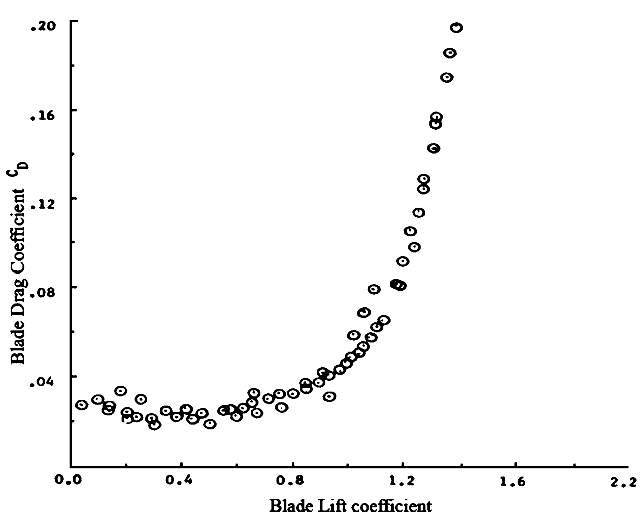

Fig. 4 Blade drag vs lift polar.

provided fairly close fit in the unstalled region, and a second-order polynomial

$$C_{\mathrm{Lb}_2} = A_3 + A_4\alpha_b + A_5\alpha_b^2, \qquad (\alpha_b > \alpha_{\mathrm{bp}}) \tag{24}$$

was sufficient to represent the data points in the stalled region. The continuity requirement at the break point is the only condition that has to be satisfied to couple these two curves.

It is required that both functions evaluated at the break point be equal, that is,

$$f\left(C_{\mathrm{Lb1}}^{(\alpha_{\mathrm{bp}})}\right) = f\left(C_{\mathrm{Lb2}}^{(\alpha_{\mathrm{bp}})}\right) \tag{25}$$

where α_{bp} is the value of α_b at the break point.

Different orders of polynomial curves ranging from 2 to 7 deg were used to represent the drag coefficient data vs blade angle-of-attack angle with the aid of a least-squares analysis. The best fit was found to be that of a second-order polynomial because of its accuracy and lower number of coefficients,

$$C_{\mathrm{Db}} = A_6 + A_7\alpha_b + A_8\alpha_b^2 \tag{26}$$

Along with the development of a propeller model, a test criterion was used to check the feasibility of the Lock's method by comparing the measured values[8] of propeller efficiency with those calculated through the application of Lock's direct method using the polynomials and coefficients defined earlier.

In-Flight Thrust Model

Rewriting the thrust and shaft power equations to include parameters of Eqs. (23) and (26) for points below the stall yields

$$T = 0.5\rho N_B C W^2 R X\Big[(A_1 + A_2\alpha_b)\cos(\phi) - \left(A_6 + A_7\alpha_b + A_8\alpha_b^2\right)\sin(\phi)\Big] \tag{27}$$

$$P_S = 0.5\rho N_B C R X V^3 \cos^2 V_C\Big\{\Big[(A_1 + A_2\alpha_b)\cos(\beta) - \left(A_6 + A_7\alpha_b + A_8\alpha_b^2\right)\sin(\phi)\Big][1 + V_C\sin(\beta)/\cos(\phi)] + V_C^{0.5}\cos(\beta)\left(A_6 + A_7\alpha_b + A_8\alpha_b^2\right)\Big\} \tag{28}$$

and for conditions above the stall,

$$T = 0.5\rho N_B C W^2 R X\Big[\left(A_3 + A_4\alpha_b + A_5\alpha_b^2\right)\cos(\phi) - \left(A_6 + A_7\alpha_b + A_8\alpha_b^2\right)\sin(\phi)\Big] \tag{29}$$

$$P_S = 0.5\rho N_B C R X V^3 \cos^2 V_C\Big\{\Big[\left(A_3 + A_4\alpha_b + A_5\alpha_b^2\right)\cos(\beta) - \left(A_6 + A_7\alpha_b + A_8\alpha_b^2\right)\sin(\phi)\Big][1 + V_C\sin(\beta)/\cos(\phi)] + V_C^{0.5}\cos(\beta)\left(A_6 + A_7\alpha_b + A_8\alpha_b^2\right)\Big\} \tag{30}$$

After verification through comparisons between the theoretical model and experimental data that the model provides satisfactory results for propeller efficiency, attention is turned to validation for calculated thrust. To validate the thrust estimation method, the following information must be available.

1) The installed propeller geometrical characteristics must include airfoil geometry at 75% of propeller radius from the hub, propeller blade radius, and number of blades.

2) The installed engine static thrust and horsepower at different throttle settings and propeller speed must be known. This information, mainly at standard sea level conditions, is available through the engine performance catalog.

3) In-flight throttle position (propeller speed in revolution per minute), indicated airspeed (IAS), indicated altitude, outside air temperature, and torque must be available. These data could be read directly from normal airplane cockpit instruments, except for piston engines, which require an extra torque meter installation.

When the listed information is assumed available for a fixed pitch propeller-driven airplane, parameters A of Eqs. (23), (24), and (26) are known through curve fitting; hence, C_{Lb} and C_{Db} are known coefficients in terms of blade angle of attack α_b.

For any throttle setting, either on the ground or flight, advance ratio J is known and propeller pitch angle θ is either measured (fixed pitch) or estimated through iteration process for variable pitch propeller type.

Blade solidity ratio is defined as

$$s = [2c/(0.75r\pi)] \tag{31}$$

Two independent values of blade lift coefficient C_{Lb}, calculated using Eq. (21) (where the value of χ is selected through a table

Table 1 Result of in-flight thrust calculation of F-27 (Friendship) airplane

	Measured data (per engine)				Predicted data (per engine)		
No.	Throttle, %	IAS, kn	RPM	Torque, psi	Torque, Psi	%Error torque	Thrust, lb
1	100	212.48	14,700	360.0	360.4	0.111	5120.2
2	85	197.25	14,000	320.5	319.2	−0.406	4810.1
3	80	187.18	13,650	N/A	312.5	N/A	4268.5
4	75	175.78	13,300	300.0	301.1	0.367	3670.0
5	70	164.12	12,800	240.5	238.8	−0.707	3125.6
6	65	158.33	12,200	200.3	200.0	−0.15	2935.9
7	60	148.76	11,800	170.7	171.1	0.234	2570.3

lookup procedure) and Eqs. (23) and (24), are compared by defining a suitable tolerance.

The initial guess for α_b could now be verified through an iteration process adopting the Newton–Raphson method to find its final value. With α_b verified, β is computed using the following equations:

$$\phi_0 = A\tan[J/(0.75\pi)] \tag{32}$$

$$\phi = \theta - \alpha_b \tag{33}$$

$$\beta = \phi - \phi_0 \tag{34}$$

Related velocities are calculated by following relations;

$$W = 0.75\cos(\beta)/\cos(\phi_0) \tag{35}$$

$$w = 0.75\sin(\beta)/[\cos(\phi_0)\cos(\phi)] \tag{36}$$

Hence thrust, torque, and shaft horse power coefficients are computed by

$$T_{\text{co}} = C_{\text{Lb}}\pi^3 W^2\cos(\phi)/8 \tag{37}$$

$$Q = (\pi^3/16)[(0.759\cos(\beta))/\cos(\phi_0)]^3 \tag{38}$$

$$A_{\text{to}} = \pi T_{\text{co}}/4 \tag{39}$$

$$F = \pi Q/4 \tag{40}$$

$$C_T = A_{\text{to}}(1 - C_{\text{Db}}\tan(\phi)/C_{\text{Lb}}) \tag{41}$$

$$C_Q = JC_T/(2\pi) + wA_{\text{to}}/2 + FsC_{\text{Db}} \tag{42}$$

$$C_P = 2\pi C_Q \tag{43}$$

Finally, the estimated values of thrust, torque, and shaft horsepower (SHP) is determined by following equations:

$$\text{SHP} = C_P\rho(\text{rpm}/60)^3(2R)^5/550 \tag{44}$$

$$\text{torque} = C_Q\rho(\text{rpm}/60)^2(2R)^5 \tag{45}$$

$$\text{thrust} = C_T\rho(\text{rpm}/60)^2(2R)^4 \tag{46}$$

This process continues for each flight condition; therefore, thrust, torque and SHP is calculated at each step as shown in flow chart of Fig. 5.

Results

The calculated values of propeller efficiency proved the accuracy of Lock's method and the propeller modeling technique by showing less than 1% error, when compared with the measured data[8] at various blade setting of 11, 13, 19, 23, and 27 deg as shown in Fig. 6.

The method has been applied for thrust calculation of a four-bladed variable pitch Rotol RA225907 propeller, installed on a twin turboprop engine of an F-27 airplane. This airplane has been tested in different throttle setting and in a wide range of its flight envelope.

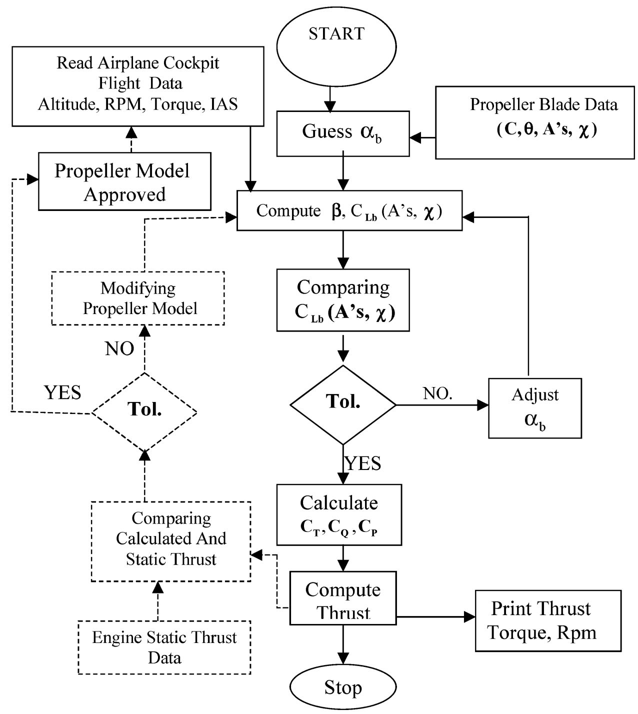

Fig. 5 Thrust calculation flow chart.

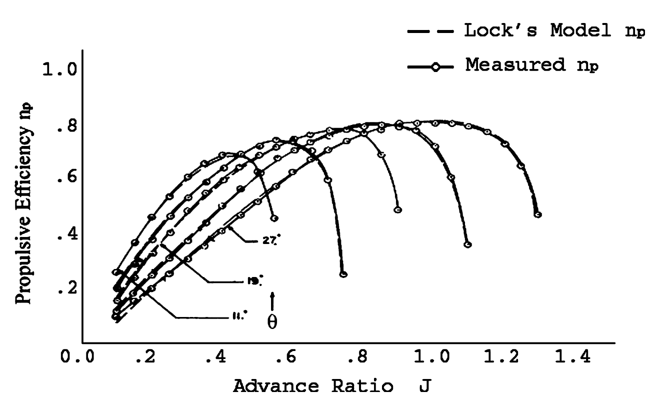

Fig. 6 Comparison of measured and calculated propulsive efficiency.

The results of curve fitting of the blade lift and drag coefficient of Rotal RA225907 propeller indicated A coefficients to be

$$C_{\text{Lb1}} = 0.4996 + 0.1096\alpha_b, \qquad (\alpha < \alpha_{\text{bp}})$$

$$C_{\text{Lb2}} = 1.3066 - 0.001\alpha_b + 0.0024\alpha_b^2, \qquad (\alpha_b > \alpha_{\text{bp}})$$

$$C_{\text{Db}} = 0.0258429 - 0.00318491\alpha_b + 0.00172721\alpha_b^2$$

When measured values of revolutions per minute and IAS at 10,000 ft, listed in Table 1, are considered to adjust blade angle of attack and engine torque values as a checkpoint to adjust its propeller pitch angle, it only took a few iterations to find predicted value of torque and its corresponding in-flight thrust at various flight conditions. Percent of error in torque estimation relative to its measured value at different flight setting is listed in Table 1.

Results of the evaluation for stopping criteria (flow chart of Fig. 5) demonstrate no sensitivity other than truncation error on the calculation process. It is recommended to set it equal to one unit of engine idle torque reading.

Conclusions

The thrust prediction method was adopted to calculate the available thrust for the purpose of flight simulation modeling. The method was validated by comparing simulated and measurement data. This comparison has shown less than 1% error in torque prediction both for ground and in-flight measurement. Static thrust results at various throttle settings also provided great accuracy, similar to that of torque results. In-flight thrust validation was based on static thrust accuracy and then on matching of engine revolutions per minute, torque, and available SHP, through which propeller pitch setting was found. Finally a validation of reliability of the in-flight thrust modeling was done by applying the thrust model on a twin engines turboprop airplane flight simulator for which complete range of flight was tested, and satisfactory results were reached.

Variation of a force parameter is well understood by any pilot or student, rather than torque or propeller speed, which do not have any reliable relation to verify airplane maneuvers or its capability. Hence, adopting of an in flight thrust measurement gage on a propeller-driven airplane to display the thrust force would certainly provide a much better feeling to pilots. Therefore, it would shorten the period of pilot training, increase the pilot's sense of available thrust, which is the most powerful tool for pilot decision making in hazardous maneuver entrance, and increase the maneuverability of existing airplanes due to lack of knowledge of available thrust during flight.

Among other benefits of installing an in-flight thrust measurement gauge, the most important beside flight safety are the increase in pilot ability in maneuvers and the possibility of using low-cost and high-maneuverability propeller-driven aircraft in close air support missions in place of jet fighter aircraft with their associated high cost and long-terms pilot training.

References

[1]Petersen, F. S., "Aircraft and Engine Performance," Naval Air Test Center, Patuxent River, MD, Spring 1958.

[2]"Hamilton Standard Method of Propeller Performance Calculation," Hamilton Standard Div. of United Aircraft Corp., East Hartford, CT, 1941.

[3]Lock, C. N. H., "A Graphical Method of Calculating the Performance of an Airscrew," British Aeronautical Research Council, ARC Rept. and Memoranda 1675, London, May 1935.

[4]Lock, C. N. H., "Application of Goldstein's Theory to the Practical Design of Airscrews," British Aeronautical Research Council, ARC Rept. and Memoranda 1377, London, Nov. 1930.

[5]Lock, C. N. H., "Tables For Use in an Improved Method of Airscrew Strip Theory Calculation," British Aeronautical Research Council, ARC Rept. and Memoranda 1674, London, Oct. 1934.

[6]Lock, C. N. H., "A Graphical Method of Calculating the Performance of an Airscrew," British Aeronautical Research Council, ARC Rept. and Memoranda 1849, London, Aug. 1938.

[7]Haines, A. B., "A Comparison of Aerofoil Data for Use in Single Radius Propeller Calculations," British Aeronautical Research Council, ARC Rept. and Memoranda 2188, London, 1947.

[8]Freeman, H. B., "Comparison of Full Scale Propeller Having R. A. F.–6 and Clark–Y Airfoil Sections," NACA Rept. 378, 1943.